

Kinetics studies of dimethyl carbonate synthesis from urea and methanol over ZnO catalyst

Junliang Zhang^{***}, Feng Wang^{*}, Wei Wei^{*†}, Fukui Xiao^{*}, and Yuhan Sun^{*}

^{*}State Key Laboratory of Coal Conversion, Institute of Coal Chemistry,
Chinese Academy of Sciences, Taiyuan 030001, P. R. China

^{**}Graduate University of the Chinese Academy of Sciences, Beijing 100039, China

(Received 6 February 2010 • accepted 6 April 2010)

Abstract—A kinetic experiment of dimethyl carbonate (DMC) synthesis by urea methanol over ZnO catalyst was carried out in an isothermal fixed-bed reactor. A kinetic model based on the mole fraction was proposed and the kinetic parameters were estimated from the experimental results. The model predictions were compared with the experimental data and fair agreements were found. The effects of the reaction temperature (443–473 K), space time (0–4.7 h mol⁻¹ kg_{cat}⁻¹) and urea mass percent (5–9%) in feed on DMC mole fraction were investigated. It was found that the reactions are mainly influenced by the reaction temperature and space time rather than urea mass percent in feed. The experimental and simulated results indicated that the reaction from MC to DMC was the rate-controlling step in the DMC synthesis process from urea and methanol. It is important to remove the DMC and byproduct ammonia to achieve a high selectivity of DMC. This implies that reactive distillation might be used in the DMC synthesis on an industrial scale to achieve a higher selectivity of DMC.

Key words: Kinetics, Dimethyl Carbonate, Methanol, Urea

INTRODUCTION

As an environmentally friendly chemical product, dimethyl carbonate (DMC) has been used widely in fields of chemical industry recently [1–5]. It can be used as carbonylation and methylation reagent to substitute extremely toxic phosgene and dimethyl sulfate. DMC can also be used as a solvent in fields such as medicine, pesticide, dyestuff and flavoring agent of foodstuff [6,7]. Moreover, DMC is an ideal additive of gasoline for its high oxygen content and high octane number [8]. Therefore, much attention has been paid to the development of a clean and simple synthesis method for DMC.

The reported methods of DMC synthesis include the reaction of phosgene and methanol, oxidative carbonylation of methanol, and ester exchange [9,10]. The traditional process of DMC synthesis via phosgene and methanol is limited in industry due to the toxic raw material involved. Currently, DMC synthesis by non-phosgene routes via the oxidative carbonylation of methanol (EniChem process and UBE process) and the transesterification method (Texaco process) are developed and applied in industry [11]. However, the drawbacks of the former method suffer from the use of poisonous or corrosive gases of carbon monoxide, hydrogen chloride and methyl nitrate and bearing the possibility of explosion [12–15]. The transesterification method is limited by the thermodynamic equilibrium conversion, which leads to low production of DMC [16,17]. Thus, in order to avoid all the shortcomings above-mentioned, a new synthesis process of DMC from methanol and urea has been investigated [18]. This process uses urea and methanol as raw material under the definite temperature, pressure with the existence of cata-

lyst. As there is no water involved during this process, the ternary azeotrope (methanol-water-DMC) does not form, the subsequent separation and purification of DMC thus can be simplified. Furthermore, the byproduct ammonia that is released during the reaction can be, in principle, recycled for urea synthesis. Therefore, this process is one kind of environment-friendly technique.

Although the synthesis of DMC by urea alcoholysis method is quite interesting, the kinetics of this process was rarely reported in the literature. Most studies focused on testing various catalysts in this process, such as bases, organotin catalysts, and metal oxides [19–25]. Very recently, Wang et al. found that ZnO showed the highest catalytic activity and stability among solid base catalysts for this process [19–22]. In this work, kinetic experiments of dimethyl carbonate synthesis from urea and methanol over ZnO catalyst were carried out in a fixed-bed reactor within the temperature range 443–473 K. A new kinetics model was developed and its parameters were determined based on the experimental results. The obtained parameters from this study will be used in the future work for modeling the DMC production.

EXPERIMENTAL

1. Materials and Catalyst Preparation

Chemicals used in this study include methanol (99.5 wt%) and urea (99.5 wt%) obtained from Tianjin University Chemical Factory (Tianjin, China). Zinc nitrate, potassium nitrate and KOH were provided by Shanghai Chemical Reagent (Shanghai, China). The preparation of ZnO catalyst was according to the method provided by Wang et al., which are shown as follows [21]: first, 2 wt% potassium nitrate aqueous solution and 80 wt% zinc nitrate aqueous solution were prepared, and their pH values were adjusted to 2.0 by KOH.

[†]To whom correspondence should be addressed.
E-mail: weiwei@sxicc.ac.cn

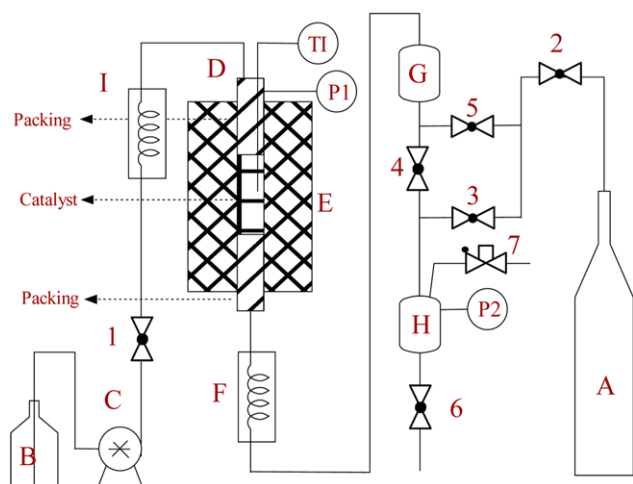


Fig. 1. Experimental setup.

- | | |
|------------------------------|---------------------------|
| Vessel and equipment | |
| A. N ₂ gas | F. Condenser |
| B. Raw liquid storage vessel | G. Surge tank |
| C. Meter pump | H. Product storage vessel |
| D. Fixed bed tubular reactor | I. Feed pre-heater |
| E. Heating furnace | |
| Valves | |
| 1-6. Glove valve | 7. Back pressure valve |

Then said solution was sprayed and impregnated on γ -alumina carrier for 1 hour by equal-volume spraying and impregnating process, respectively, and the carrier with active component supported thereon was then dried at 423 K for 8 hours and calcined at 1,073 K for 8 hours. The prepared catalyst was composed of potassium oxide (2 wt%), zinc oxide (31 wt%) and Al₂O₃ (67 wt%). The specific surface area of the sample, which was determined by BET method with a Micromeritics ASAP-2000, was 72.3 m²/g.

2. Experimental Procedure

The experimental equipment (as shown in Fig. 1) was a stainless fixed bed tubular reactor with a pre-heater, a product condenser, a stuff storage vessel of 500 mL and two product storage vessels of 2,000 mL. The pipes of the apparatus were traced to maintain the desired temperature. 2.0 g catalyst was charged into the reactor (ID=10 mm), and the residues zone of the reactor was filled with inert bead. The reactor was housed in an electric furnace controlled by a programmable temperature controller. The temperature of the catalyst bed was measured by a sliding thermocouple placed at the center of the catalyst bed. N₂ was introduced into the reactor and compressed to a desired pressure prior to reaction. The pressure of the reactor was controlled by a back-pressure regulator. The reactants were heated to the desired temperature in the pre-heater and then continuously fed into the reactor by a meter pump. The reaction products were cooled to 60 °C in the product condenser and then entered into the product storage vessel. After reaching steady state at the designated temperature, samples were taken at intervals of 3 hours. The compositions of the liquid samples were detected by a GC-950 gas chromatograph (GC) equipped with Porapak-Q column of 2,000 mm in length and 4 mm in diameter with TCD as detector. The gas chromatograph applied a temperature ramp for the analysis: the column temperature was kept at 80 °C for 3 min, and then the temperature was raised 20 °C per minute until a tem-

perature of 200 °C was reached. The temperature was maintained for ten minutes before the column oven was cooled to 80 °C for the next analysis.

The kinetics of DMC synthesis was studied at seven different temperatures (443, 448, 453, 458, 463, 468 and 473 K). At each reaction temperature, the space time was varied in the range of 0.1–4.7 [h mol⁻¹ kg_{cat}] by changing the liquid feed rate. The space time, τ , of reactants with catalyst is defined as

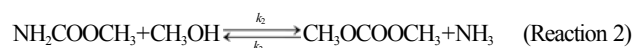
$$\tau = W_{cat}/F \quad (1)$$

Where W_{cat} is the amount of catalyst, F is the mole flow rate of feed. All the experiments were operated at 1.2 MPa with 5 wt% urea in feed.

RESULTS AND DISCUSSION

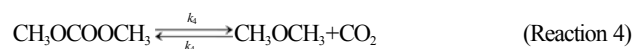
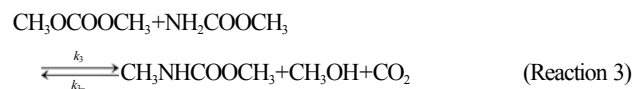
1. Kinetics Model

Wang et al. and Zhao et al. studied the synthesis of DMC from urea and methanol over zinc compounds and observed that in the synthesis of DMC from urea and methanol, the following sequence of reactions took place [20–24,26]:



The reaction of urea to DMC can be divided into two steps: first, methyl carbamate (MC) is synthesized from urea and methanol (see reaction 1); secondly, MC further reacts with methanol to produce DMC (see reaction 2).

Besides the above two main reactions (reaction 1 and 2), there were other side reactions in urea methanolysis. In our previous work, *N*-methyl methyl carbamate (NMMC) was detected as the major byproduct, which can be formed from DMC and MC (see reaction 3). In addition, Fu et al. reported that DMC was prone to thermal decomposition over ZnO [27]. Ono et al. revealed further that DMC could be decomposed to dimethyl ether and carbon dioxide in the presence of metal oxides (see reaction 4) [28].



Considering the reactions 1–4, the reaction rate of each component can be described as follows:

$$\frac{dx_{MeOH}}{d\tau} = -r_1 - r_2 + r_3 \quad (2)$$

$$\frac{dx_{Urea}}{d\tau} = -r_1 \quad (3)$$

$$\frac{dx_{DMC}}{d\tau} = r_2 - r_3 - r_4 \quad (4)$$

$$\frac{dx_{MC}}{d\tau} = r_1 - r_2 - r_3 \quad (5)$$

$$\frac{dx_{NMMC}}{d\tau} = r_3 \quad (6)$$

$$\frac{dx_{CO_2}}{d\tau} = r_3 + r_4 \quad (7)$$

$$\frac{dx_{NH_3}}{d\tau} = r_1 + r_2 \quad (8)$$

$$\frac{dx_{DME}}{d\tau} = r_4 \quad (9)$$

Where τ denotes the space time.

According to the above-mentioned reaction pathway, the expressions of reaction rate in term of mole fraction can be defined as follows:

$$r_1 = W_{cat} k_1 \left(x_{urea} x_{MeOH} - \frac{1}{K_{eq,1}} x_{MC} x_{NH_3} \right) \quad (10)$$

$$r_2 = W_{cat} k_2 \left(x_{MC} x_{MeOH} - \frac{1}{K_{eq,2}} x_{DMC} x_{NH_3} \right) \quad (11)$$

$$r_3 = W_{cat} k_3 \left(x_{DMC} x_{MC} - \frac{1}{K_{eq,3}} x_{NMMC} x_{CO_2} x_{MeOH} \right) \quad (12)$$

$$r_4 = W_{cat} k_4 \left(x_{DMC} - \frac{1}{K_{eq,4}} x_{DMC} x_{CO_2} \right) \quad (13)$$

Where x_j is the mole fraction of species j (MeOH, urea, DMC, MC, NMMC, CO_2 , NH_3 , or DME), k_j is the forward reaction rate constants of reaction i ($i=1-4$) and W_{cat} is the amount of catalyst, $K_{eq,i}$ is the chemical equilibrium constants ($K_{eq,i} = k_f/k_r$).

Our previous studies have verified that reactions 1-4 represent elementary reaction steps [19,21,22]. The relations of the chemical equilibrium constants $K_{eq,i}$ with temperature ranging from 300-600 K determined by Wang et al. are represented in Table 1 [20]. From the table, the equilibrium constant is not very high for reaction 1 and not very low for reactions 2 and 3 in the temperature range of 300-600 K. However, the equilibrium constant is very high for reaction 4. Hence, Eq. (13) can be simplified as the following form:

$$r_4 = W_{cat} k_4 k_{DMC} \quad (14)$$

The relationship of equilibrium constant and temperature in Table 1 is explained by the van't Hoff equation (Eq. (15)):

$$\ln K_{eq,i} = -\frac{(\Delta_r H)_i}{R_g T} + \frac{(\Delta_r S)_i}{R_g} \quad (15)$$

where $(\Delta_r H)_i$ is the standard enthalpy change of the reaction, $(\Delta_r S)_i$

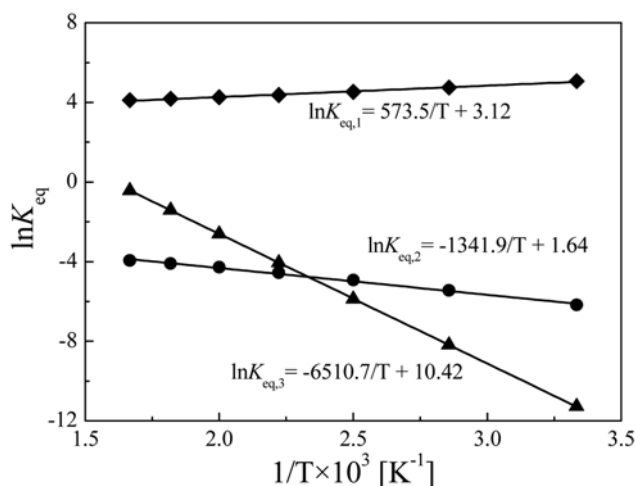


Fig. 2. Van't Hoff plots for $K_{eq,1}$, $K_{eq,2}$ and $K_{eq,3}$.

is standard entropy change of the reaction, and R_g the universal gas constant.

The linearization of $\ln K_{eq,i}$ with $1/T$ is shown in Fig. 2 and the following equations are obtained from the plots:

$$\ln K_{eq,1} = 573.5/T + 3.12 \quad (16)$$

$$\ln K_{eq,2} = -1341.9/T + 1.64 \quad (17)$$

$$\ln K_{eq,3} = -6510.7/T + 10.42 \quad (18)$$

2. Kinetic Parameter Determination

For the optimization, a Matlab program was employed to find the best-fitted reaction rate constants which minimize the relative

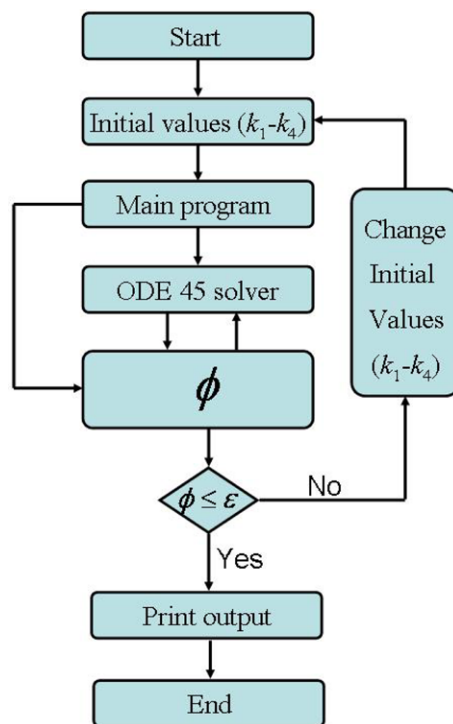


Fig. 3. Optimization algorithm for reaction rate constants estimation.

Table 1. Dependence of the equilibrium constant on temperature

| Temperature [K] | Reaction equilibrium constant | | | |
|--------------------|-------------------------------|------------|------------|------------|
| | $K_{eq,1}$ | $K_{eq,2}$ | $K_{eq,3}$ | $K_{eq,4}$ |
| 300 | 158.88 | 2.07E-03 | 1.27E-05 | 3.22E+08 |
| 350 | 114.79 | 4.31E-03 | 2.76E-04 | 2.10E+08 |
| 400 | 92.30 | 7.19E-03 | 2.82E-03 | 1.53E+08 |
| 450 | 79.19 | 1.04E-02 | 1.73E-02 | 1.19E+08 |
| 500 | 70.79 | 1.37E-02 | 7.39E-02 | 9.63E+07 |
| 550 | 65.03 | 1.66E-02 | 2.42E-01 | 8.05E+07 |
| 600 | 60.90 | 1.92E-02 | 6.52E-01 | 6.88E+07 |

root mean square deviation values expressed by Eq. (19):

$$\phi = \frac{1}{n} \sqrt{\sum_{m=1}^n \left(\frac{x_{j,pred,m} - x_{j,exp,m}}{x_{j,exp,m}} \right)^2} \quad (19)$$

where $x_{j,pred}$ and $x_{j,exp}$ are the predicted and experimental mole fractions of the component j , respectively. Fig. 3 illustrates the proposed algorithm for obtaining kinetic constants (k_i). The solver ODE45 was used to solve the series of above ordinary differential equations. The algorithm first estimates the parameters (k_i – k_4) followed by solving the ordinary differential equations and checking the error between results and the experimental data. The process continues until convergence to the experimental data is reached. The k_i values at the different temperature are calculated from the regression equation, as are shown in Table 2. It is obvious that the reaction temperature has a strong effect on the reaction rate constants.

The relationship of reaction rate constants k_i and the absolute temperature obeys the Arrhenius equation:

$$k_i = A_i \exp(-E_{a,i}/R_g T) \quad (20)$$

Where k_i is the reaction rate constants, $E_{a,i}$ the apparent activation energies, A_i the constant called the pre-exponential factor, and T the Kelvin temperature.

Take logarithm with Eq. (20):

Table 2. The values of reaction rate constants at different temperature

| Temperature [K] | Reaction rate constants [mol h ⁻¹ kg _{cat} ⁻¹] | | | |
|--------------------|--|--------|---------|--------|
| | k_1 | k_2 | k_3 | k_4 |
| 443 | 9760.22 | 0.0779 | 13.0987 | 0.0264 |
| 448 | 10975.05 | 0.0947 | 18.0099 | 0.0287 |
| 453 | 11404.58 | 0.1087 | 22.8324 | 0.0372 |
| 458 | 11455.55 | 0.1393 | 26.3830 | 0.0448 |
| 463 | 14238.15 | 0.1944 | 30.5285 | 0.0649 |
| 468 | 16863.89 | 0.2762 | 35.4414 | 0.0727 |
| 473 | 22000.49 | 0.3608 | 41.0217 | 0.1114 |

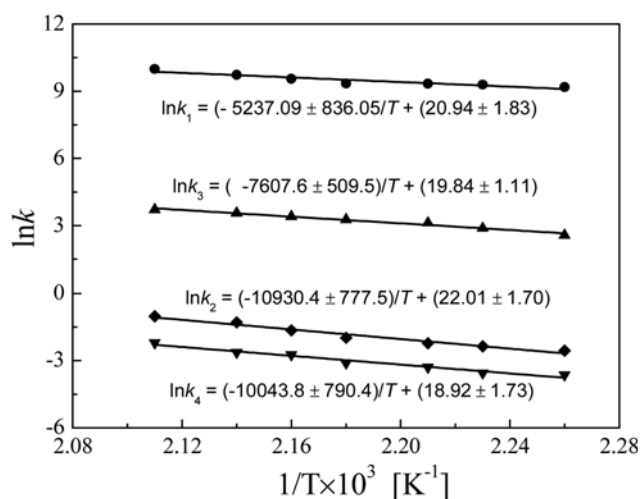


Fig. 4. Arrhenius plots (Marks indicate fitted k_i values derived from kinetic experiments) Amount of catalyst: 2.0 g; Feed composition: 5 wt% urea+95 wt% methanol.

Table 3. Pre-exponential factors and activation energies

| Reaction rate constant k [mol h ⁻¹ kg _{cat} ⁻¹] | Pre-exponential factor A [mol h ⁻¹ kg _{cat} ⁻¹] | Activation energy E_a [kJ mol ⁻¹] | Variance R^2 |
|--|--|--|-------------------|
| k_1 | 1.24×10^9 | 43.54 | 0.864 |
| k_2 | 3.63×10^9 | 90.87 | 0.964 |
| k_3 | 4.14×10^8 | 63.25 | 0.973 |
| k_4 | 1.65×10^8 | 83.50 | 0.962 |

$$\ln k_i = -\frac{E_{a,i}}{R_g T} + \ln A_i \quad (21)$$

The relationship between $\ln k_i$ and $1/T$ is shown in Fig. 4 and is treated by the linear regression method. The pre-exponential factors and activation energies were obtained by plotting $\ln k_i$ versus $1/T$, and the results are listed in Table 3. The obtained activation energies of different reactions have a range of 43.54 to 90.87 kJ mol⁻¹; among them, the activation energy of the MC to DMC is the highest (90.87 kJ mol⁻¹) and that of the DMC to DME is the second highest (83.50 kJ mol⁻¹). These are remarkably higher than the values of the other reactions (43.54 and 63.25 kJ mol⁻¹). This fact shows that the reaction rates of reactions (2) and (4) are more sensitive to the temperature variation than those of reactions (1) and (3).

The experimental results at different reaction temperatures together with the accompanying theoretical predictions are given in Fig. 5(a)-(d) using the fitted kinetics parameters and chemical equilibrium constants $K_{eq,j}$. The lines in Fig. 5(a)-(d) are the calculated mole fraction results by the above kinetics model with the kinetics parameters presented in Table 3. All the marks in Fig. 5(a)-(d) are the experimental mole fractions of four components at different temperatures.

It can be seen from Fig. 5(a)-(d) that the simulated results from the kinetics model match the experimental ones very well, which suggests that the proposed reaction rate model is well suited to reproduce the experimental results. This point makes it possible to investigate the corresponding reaction rates at various urea mass percents. The effect of urea mass percents in the feed on the mole fraction of DMC is shown in Fig. 6. It can be seen that urea mass percents in the feed have only a slight influence on the mole fraction of DMC in the products when the urea mass percent ranges between 5% and 9%. However, the required time to reach the equilibrium of reaction (2) decreases with the increase of urea mass percent.

The effect of space time on DMC mole fraction in the product at different temperatures (ranging from 443 to 473 K) is shown in Fig. 5(a). The change of DMC mole fraction with space time at different reaction temperatures shows similar trends. The DMC mole fraction increased with space time firstly and then leveled off. This may result from the fact that the byproduct ammonia restricted the reaction shift from MC to DMC. Hence, the byproduct ammonia should be removed in time in order to shift the reaction equilibrium.

The effects of space time on the mole fractions of NMMC and DME are shown in Fig. 5(b) and (c), respectively. It can be seen from the figures that the change of NMMC mole fraction with space time show similar trends as that of DME mole fraction. At the same reaction temperature, the mole fraction of NMMC and DME increased monotonically with the increase of space time. A higher

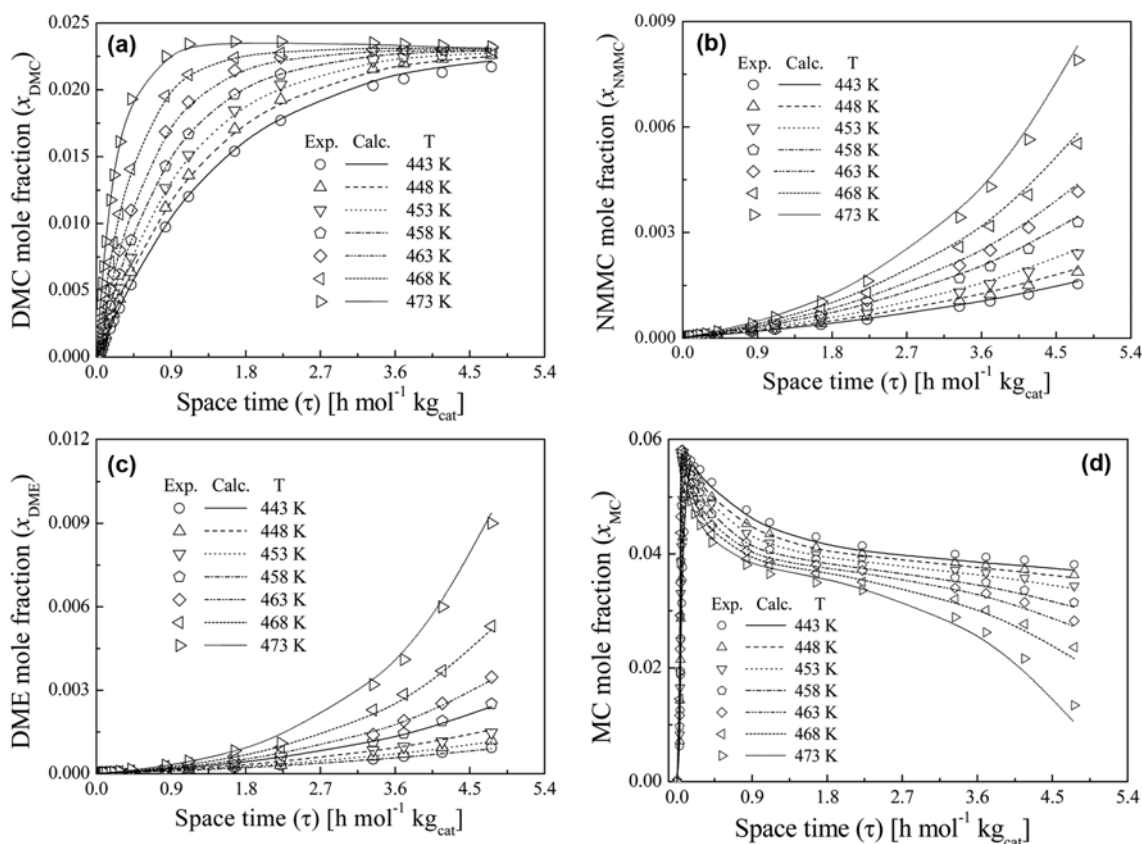


Fig. 5. Mole fractions of DMC (a), NMMC (b), DME (c) and MC (d) as a function of space time at different temperatures.

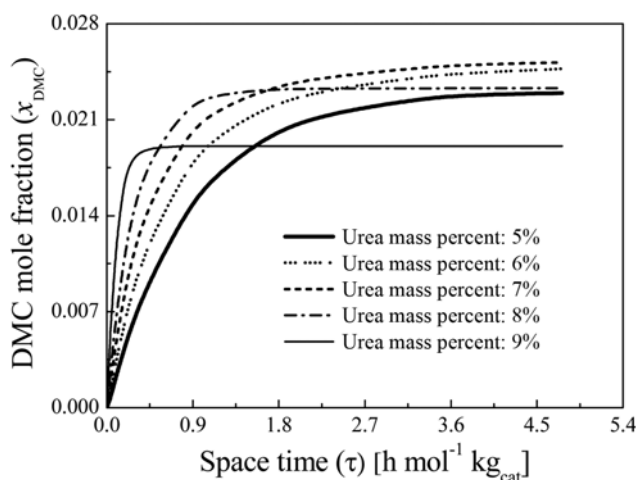


Fig. 6. Model prediction: DMC mole fraction as a function of space time for different urea mass percents in feed at 458 K.

reaction temperature accelerated the rate of side reactions. As both side reactions consumed DMC, removing DMC from the reaction system in time could restrain the side reactions. Therefore, a catalytic distillation technique was introduced into the DMC synthesis to solve the problems in unfavorable equilibrium and complicated side reactions.

The effect of the space time on MC mole fraction is shown in Fig. 5(d). The MC mole fraction increased linearly with the space

time for the first few hours. As the reaction progressed, the MC mole fraction reached a maximum and then decreased sharply. By comparing the result in Fig. 5(a) and 5(d), an important phenomenon was observed: the mole fraction of MC was significantly higher than that of DMC under the same reaction conditions. This indicated that the intermediate MC was easily prepared, but was difficult to convert into DMC. Therefore, reaction 2 from MC to DMC was the rate-controlling step in DMC synthesis. The key to promoting DMC yield was to find a proper catalyst to shift the reaction from MC and methanol to the DMC. Besides, when the space time was higher than $2.7 \text{ h mol}^{-1} \text{kg}_{\text{cat}}^{-1}$, the MC mole fraction decreased sharply under high reaction temperature (in Fig. 5(d)); however, DMC mole fraction almost remained constant (in Fig. 5(a)). This indicated that the formation rate of DMC was almost equal to the consumption rate under the above-mentioned conditions.

CONCLUSIONS

Detailed kinetics experiments and models for the reaction system from urea and methanol to yield DMC over ZnO catalyst have been developed. This reaction system was considered to include two main reactions and two side reactions. The effect of temperature, space time and urea mass percent in feed on the mole fraction of DMC were studied. The reaction rate constants at different temperatures are fitted by applying a Matlab program to minimize the relative root mean square deviation values. The apparent activation energies and the pre-exponential factors of DMC synthesis process

were determined by the Arrhenius equation based on the relationship of reaction rate constants and temperature (ranging from 443 K to 473 K). The experimental mole fractions of DMC, MC, NMMC and DME as a function of temperature and space time were fitted well with the corresponding theoretical predictions using the fitted kinetics parameters and chemical equilibrium constants $K_{eq,i}$.

Experimental results indicated that reaction 2 from MC to DMC was the rate-controlling step in DMC synthesis. It seemed necessary to remove DMC and ammonia from the reaction mixture for two reasons: first, the removal of DMC and ammonia could enhance the DMC yield by shifting the equilibrium of reaction (2); secondly, removing DMC from the reaction system in time was important to restrain side reactions.

Reactive distillation might be used in a DMC synthesis system on an industrial scale to achieve a higher selectivity of DMC. It is expected that the kinetics parameters presented in the paper could be used in the modeling of a reactive distillation processes.

ACKNOWLEDGEMENT

The authors would like to acknowledge the financial support from the State Key Program for Development and Research of China (No. 2006BAC02A08).

NOMENCLATURE

- A_i : pre-exponential factor [$\text{mol h}^{-1} \text{kg}_{cat}^{-1}$]
 E_a : apparent activation energy [kJ mol^{-1}]
 F : mole flow rate of feed [mol h^{-1}]
 $(\Delta H)_i$: standard enthalpy change of the reaction [kJ s^{-1}]
 $K_{eq,i}$: chemical equilibrium constant
 k_i : forward reaction rate constant of reaction i [$\text{mol h}^{-1} \text{kg}_{cat}^{-1}$]
 k_{i-} : backward reaction rate constant of reaction i [$\text{mol h}^{-1} \text{kg}_{cat}^{-1}$]
 R_g : gas constant ($=8.314$) [$\text{J mol}^{-1} \text{K}^{-1}$]
 r_i : reaction rate [mol h^{-1}]
 $(\Delta_r S)_i$: standard entropy change of the reaction [$\text{J mol}^{-1} \text{K}^{-1}$]
 T : reaction temperature [K]
 W_{cat} : amount of catalyst [kg]
 $x_{j,exp}$: experimental mole fraction
 $x_{j,pred}$: predicted mole fraction
 x_j : mole fraction of component j

Greek Symbol

- τ : space time, W_{cat}/F [$\text{h mol}^{-1} \text{kg}_{cat}$]
 ϕ : relative root mean square deviateon

REFERENCES

1. D. Delledonne, F. Rivetti and U. Romano, *Appl. Catal. A. Gen.*, **221**, 241 (2001).
2. Y. Ono, *Appl. Catal. A. Gen.*, **155**, 133 (1997).
3. F. Rivetti, *Stud. Surf. Chem. Catal.*, **3**, 497 (2000).
4. P. Tundo and M. Selva, *Accounts Chem. Res.*, **35**, 706 (2002).
5. X. Wang, S. Yan, Z. Li, K. Fan, M. Kang and S. Peng, *Korean J. Chem. Eng.*, **21**(2), 378 (2004).
6. D. Kanne, Diane, US Patent, 5,004,480 (1991).
7. H. C. Shiao, D. Chua, H. P. Lin, S. Slane and M. Salomon, *J. Power Sources*, **87**, 167 (2000).
8. M. A. Pacheco and C. L. Marshall, *Energy Fuel*, **11**, 2 (1997).
9. N. S. Isaacs, B. O'Sullivan and C. Verhaelen, *Tetrahedron*, **55**, 11949 (1999).
10. T. Sakakura, J. C. Choi and Y. Saito, *Polyhedron*, **19**, 573 (2000).
11. T. Wei, M. Wang, W. Wei and Y. Sun, *Green Chem.*, **153**, 41 (2004).
12. H. Itoh, Y. Watanabe, K. Mori and H. Umino, *Green Chem.*, **5**, 558 (2003).
13. R. Jiang, S. Wang, X. Zhao, Y. Wang and C. Zhang, *Appl. Catal. A. Gen.*, **238**, 131 (2003).
14. U. Romano, R. Tesel, M. M. Mauri and P. Rebora, *Ind. Eng. Chem. Prod. Res. Dev.*, **19**, 396 (1980).
15. Y. Yamamoto, T. Matsuzaki, S. Tanaka, K. Nishihira, K. Ohdan, A. Nakamura and Y. Okamoto, *J. Chem. Soc., Faraday Trans.*, **93**, 3721 (1997).
16. B. M. Bhanage, S. Fujita, Y. Ikushima, K. Torii and M. Arai, *Green Chem.*, **5**, 71 (2003).
17. T. Wei, M. Wang, W. Wei, Y. Sun and B. Zhong, *Fuel Process Technol.*, **83**, 175 (2003).
18. P. Ball, H. Fuellmann and W. Heitz, *Angew. Chem., Int. Ed.*, **19**, 718 (2003).
19. M. Wang, N. Zhao, W. Wei and Y. Sun, *Ind. Eng. Chem. Res.*, **44**, 7596 (2005).
20. M. Wang, H. Wang, N. Zhao, W. Wei and Y. Sun, *Ind. Eng. Chem. Res.*, **46**, 2683 (2007).
21. M. Wang, N. Zhao, W. Wei and Y. Sun, *Stud. Surf. Sci. Catal.*, **153**, 197 (2004).
22. M. Wang, H. Wang, N. Zhao, W. Wei and Y. Sun, *Catal. Commun.*, **7**, 6 (2006).
23. W. Zhao, F. Wang, W. Peng, N. Zhao, J. Li, F. Xiao, W. Wei and Y. Sun, *Ind. Eng. Chem. Res.*, **47**, 5913 (2008).
24. B. Yang, P. Wang, H. Lin, J. Sun and X. Wang, *Catal. Commun.*, **7**, 472 (2006).
25. H. Ju, M. D. Manju, K.-H. Kim, S.-W. Park and D.-W. Park, *Korean J. Chem. Eng.*, **24**(5), 917 (2007).
26. S. A. Anderson, S. Manthata and T. W. Root, *Appl. Catal. A. Gen.*, **280**, 117 (2005).
27. Y. Fu, H. Zhu and J. Shen, *Thermochim. Acta*, **434**, 88 (2005).
28. E. Suzuke, M. Akiyama and Y. Ono, *Chem. Commun.*, 136 (1992).